école normale supérieure paris-saclay

NeuroPoly

PRE-DOCTORAL RESEARCH YEAR (ARPE) REPORT

Estimation of spinal cord symmetry from MRI data to improve registration algorithms

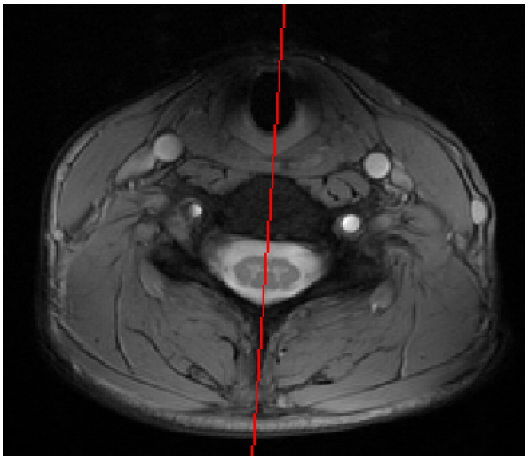

Nicolas Pinon
2018-2019

Supervisor : Julien Cohen-Adad

Contents

1 Introduction

The aim of this report is to present the work I have been doing since October in my internship at the Neuropoly research laboratory.
I will briefly introduce the social context in which I have been working and the scientific context of my research. Then I will state the problem I am working on and present the state-of-the-art methods used to solve problems close to mine. After that I will present my work and contribution in solving the problem. Then I will present ideas to continue and improve my work and what can be done next. I will finish the report with a personnal conclusion on this research year abroad.

1.1 Objectives and environment presentation

The main objective of this pre-doctoral research year is to gain knowledge in the internship's subject field, here image processing applied to medical imaging and Magnetic Resonance (MR) imaging, to pursue an autonomous research activity and to discover the research environment in a foreign country.

The research laboratory in which I work is named Neuropoly[1] and is part of Polytechnique Montreal, in Quebec. The laboratory focuses on *Magnetic Resonance Imaging* (MRI), on various aspects :

- Hardware design (coil, "magnets")
- MRI sequences
- Post-processing of the images (segmentation, registration, etc.)
- Clinical studies (mostly on multiple sclerosis)

The professor who supervises me is Julien Cohen-Adad[2], an MR physicist specialised in quantitative assessment of the brain and spinal cord structure and function.

[1] `https://www.neuro.polymtl.ca/home`
[2] `https://www.polymtl.ca/expertises/en/cohen-adad-julien`

1.2 Magnetic Resonance Imaging

1.2.1 Nuclear Magnetic Resonance

We will present a quick, simple and classical[3] description of NMR, for a more in-depth understanding of this phenomenon please refer to [1].

Atoms with an odd number of protons and/or an odd number of neutrons possess a nuclear *spin* angular momentum, which is a necessary condition to exhibit the NMR phenomenon.
We can visualize the nuclear spins as spinning charged spheres that give rise to a small magnetic moment, for instance, the hydrogen nucleus figure 1.

Figure 1: We can visualise the Hydrogen atom as a charged sphere spinning, that give rise to a small magnetic moment (in yellow) [9]

At first, all the spins in the object of study are oriented quite randomly, we then put them in a static magnetic field, which we name B_0, and which by convention is oriented in what we will define as the z direction. The spins will start to align in the z direction and the sum exhibit a net magnetic moment noted $\boldsymbol{M}$:

$$\boldsymbol{M} = \begin{bmatrix} 0 \\ 0 \\ M_0 \end{bmatrix}$$

We can see an illustration of this phenomenon figure 2. We can visualize this as a spinning-top rotating around the axis of gravity, here the spinning-top being the spin and the field of gravity being the static magnetic field.

[3] as opposed to a quantum mechanical description

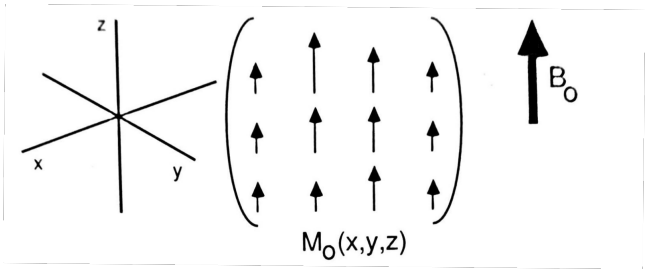

Figure 2: The spins get aligned with the static field B_0 [2]

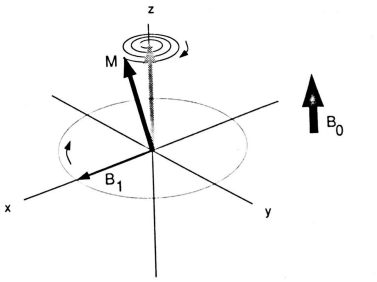

Figure 3: $\boldsymbol{M}$ is being tipped by the $\boldsymbol{B_1}$ field and exhibits the precession phenomenon [2]

To continue with the spinning-top analogy, it is difficult to visualize the spinning-top rotation speed if it is aligned with the gravitational field, i.e. if the spinning top is upright. However, if we tip the spinning-top a little-bit, it will start to exhibit a *precession* phenomenon as we can see figure 4. This precession phenomenon allows us to "see" the rotating speed of the spinning top.

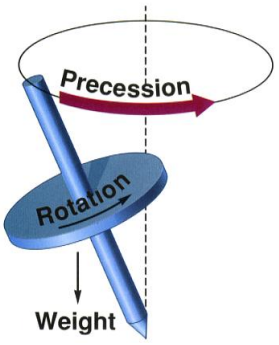

Figure 4: Spinning-top exhibiting the precession phenomenon [22]

For the actual spins, this "tipping" of $\boldsymbol{M}$ will be done by another magnetic field (this time not static), which we name B_1 and which is in the xy plane, see figure 3. After the "tipping", the spins will precess around the z axis at a well defined frequency called the *Larmor frequency* :

$$\omega = \gamma B_0$$

Where $\omega = 2\pi f$, with f the frequency of the rotation and γ being the *gyromagnetic ratio*, a known constant unique for each type of atom. In MRI, most of the time

we are imaging the hydrogen atom, H^1, because it is very abundant in the human body (composed of 70% of H_2O). Thus γ is constant, and roughly equal to 267.5 $10^6 \text{rad} \cdot \text{s}^{-1} \cdot \text{T}^{-1}$

After $\boldsymbol{M}$ has been tipped, it will exhibit a relaxation phenomenon, as we can see figure 5. This relaxation can be separated into two different but related phenomena:

- Longitudinal relaxation, characterized by a time constant T1, which is the amount of time M_z (the longitudinal component of $\boldsymbol{M}$) will take to regrow to M_0.
- Transverse relaxation, characterized by a time constant T2, which is the amount of time M_{xy} (the transverse component of $\boldsymbol{M}$) will take to return to 0.

It appears rather clearly that any longitudinal relaxation contributes to transverse relaxation, therefore $T1 \geq T2$.

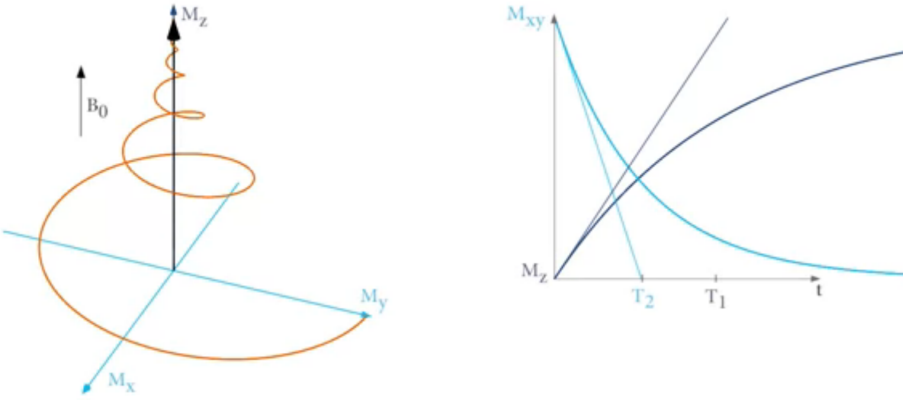

Figure 5: On the left the relaxation phenomenon with $\boldsymbol{M}$ in orange and on the right the plot of the longitudinal and transverse component of $\boldsymbol{M}$[23]

These two relaxation phenomena will lead to the production of contrast in the image, but the formation of the image is a much more complex subject, the interested reader can refer to [2]

We will not describe the NMR phenomenon any further, the reader must keep in mind that this phenomenon is complex and we recommend refering to appropriate literature (for instance [1]) to learn more about it.

1.2.2 Image contrasts

As previously stated, the two main parameters of the spin relaxation are T_1 and T_2. These two parameters will lead to the two basic image contrast that we can encounter in MR imaging : T1 weighting (T1w) and T2 weighting (T2w). Here the term "weighting" means that each voxel of the image is weighted somehow by T1 or T2, the voxel intensity does not represent the "true value" of T1 or T2 neither is it proportional directly to T1 or T2[4]

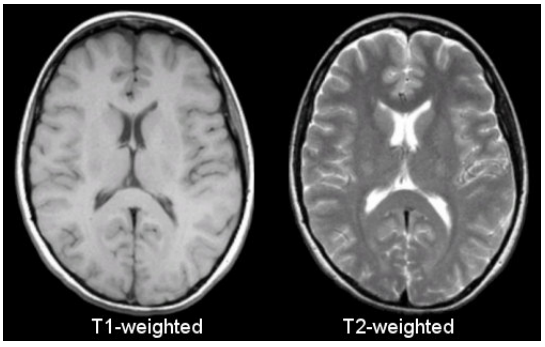

Figure 6: Two images of the brain in the transverse plane, one weighted by T1 and the other by T2 [24]

We can clearly see on the figure 6 that the same structure appears but with different contrast.

Overall, MR imaging is quite diverse, and there is many more image contrasts than just T1 and T2, such as Proton Density (PD), Magnetisation Transfer (MT) and many more. There are many parameters we can play with when recording the MR signal, thus leading to many different contrasts. Even T1w and T2w are not an absolute definition and the image can vary depending on the *sequence*[5] applied.

We shall end our short description of MRI here, for a more detailed introduction to its principles and resulting images contrasts, please refer to [2]

[4]Most of the time the weighting of the voxel is proportional to an $e^{-T_{\{1,2\}}}$ and often the voxel is affected by both parameters (and others), one is just more prevalent than the other, rendering the other negligible

[5]An MRI sequence is a particular arrangement of acquisition parameters leading to a particular image appearance

1.3 Brief overview of the spinal cord anatomy and physiology

We will give in this section a brief anatomical and physiological overview of the spinal cord, because it is the part of the body we will be imaging and thus work on in this report.

The spinal cord is one of the two part of the *central nervous system*, the other one being the brain. The central nervous system role is to process the information received from the nerves and to use this information to coordinate all parts of the body.
If we were to simplify the functioning of the whole system, we could say that the brain is the part that process the information and the spinal cord is the part that sends and receives the electrical nervous signals. In reality the role of the spinal cord is a bit more complex, involving complex processing circuits included in the grey matter.

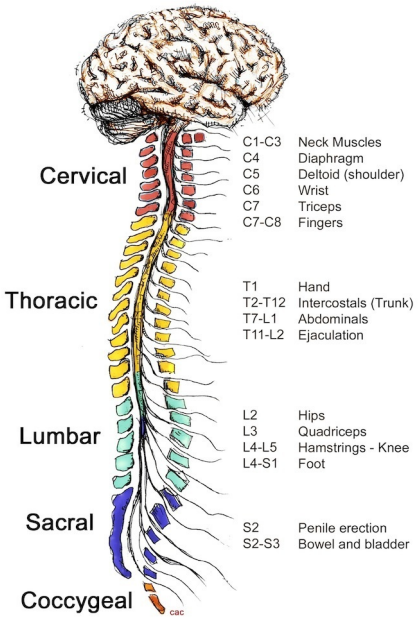

Figure 7: Decomposition of the spinal cord into its 31 segments and the organs each approximately controls [26]

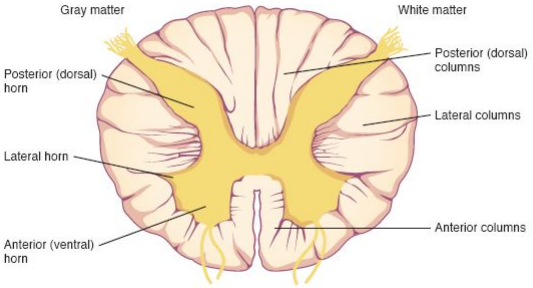

Figure 8: transverse view and anatomical annotation of the spinal cord [25]

The spinal cord is on average 44 cm long and the width on average ranges from 6.4

mm to 13 mm. It is divided into 31 segments that are detailed on figure 7. The spinal cord is enclosed in the vertebral column (a series of bones named vertebrae). The spinal cord is made of two tissues : white matter and grey matter. Between the vertebral column and the spinal cord lies a fluid, the cerebro-spinal fluid. As one can notice, except the vertebral column, those structure (white, gray matter, cerebro-spinal fluid, etc.) are the same in the brain. This is because both are joined and form one entity : the central nervous system. Also, the spinal cord consists of many tracts, which goal is to send the sensory informations from the nerves to the brain (ascending tracts) and to send the motor signals from the brain to the muscle (descending tracts).

We can view a simple anatomical description on a transverse slice of the spinal cord on figure 8.

For a more detailed introduction on spinal cord anatomy and physiology, please refer to [4].

1.4 The spinal cord toolbox

The overall frame in which my research is included in is the Spinal Cord Toolbox (SCT) [6]. Nowadays the post-processing part of the analysis of medical images is becoming more and more important, tasks such as segmentation or registration are an important part of, for instance, longitudinal studies.

Reproducibility is one of the cornerstone of science, however on 1576 researchers surveyed by *Nature* in 2016, around 90% think that there is a reproducibility crisis [5]. In this context, the development of open-source tools is crucial to the medical imaging community.

SCT's goal is to provide the medical community tools to process spinal cord MRI data, like FreeSurfer, SPM, FSL and BrainVoyager do for the brain. Before SCT, no tools were available for such processing and thus, research teams had to come up with home-made algorithms, leading to a lack of reproducibility.

Figure 9: SCT's logo [6]

SCT not only integrates existing algorithm but the laboratory actively creates new algorithms or adapt them to the specific case of spinal cord MRI.

Tools available in SCT include :

- Automatic segmentation of the spinal cord
- Automatic segmentation of the spinal canal (which includes the cord and CSF)
- Automatic segmentation of the white and gray matter using multi-atlas algorithm
- Automatic vertebral labeling
- MRI template of the human spinal cord
- Probabilistic template of white and gray matter
- Atlas of white matter tracts
- Probabilistic map of spinal levels
- Robust motion correction methods for diffusion and functional MRI time series
- Pipeline for registering data with the template
- Pipeline for registering multiple data with different acquisition parameters

The tools and algorithms in SCT heavily rely on applied-mathematics techniques and machine learning.

The focus on this report will be on the two last tools, which have in common a key concept in image processing : *registration*.

1.5 Registration

1.5.1 Definition

Previously we specified that there exist many different image contrasts in MRI (T1w, T2w and so on). For instance, when acquiring a T1w and then a T2w of the same subject, it is likely that the subject has moved in-between the two acquisitions. Therefore, if we want to accurately compare the two images, we must "align" them together, i.e. moving one image to match the other. This process is known as *registration*.

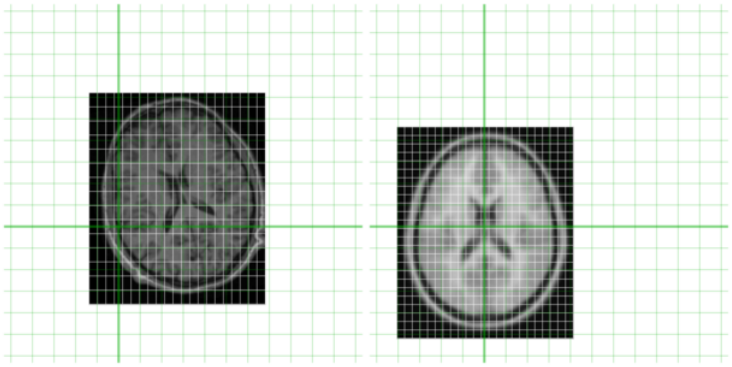

Figure 10: Two MRI transverse slices of the brain [27]

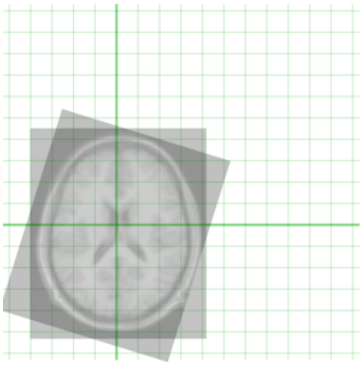

Figure 11: The two MRIs have been registered

In the simplest case, registration consists only of a translation. We can add a rotatation after the translation to register the images more precisely. Registrations done only by translation and rotation are named *rigid* registrations. To fine-tune the registration, we can add *shearing* to the registration to obtain an even more precise alignment.

These registrations are all linear, because we can describe them with basic linear algebra tools. More complex registration can be done by using non-linear transformation, that we shall present later.

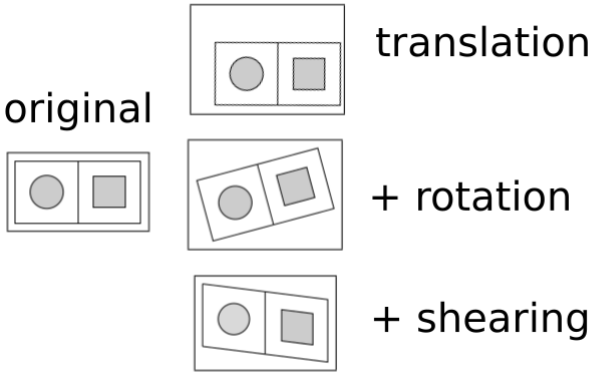

Figure 12: Different types of linear transformations [28]

1.5.2 Application

We stated an example of registration usefulness previously, but we wish to give a more complete list of the applications of registration :

- Comparing images with the same sequence taken at different times, for instance if a patient takes a particular sequence of MRI one day, and do the exact same sequence another day, registration is useful to compare the evolution of the patient.
- Comparing images with the same sequence taken from different subjects. This can be useful in studies where we wish to analyze a specific feature, for instance the white/grey matter ratio across subjects. In these studies we wish to normalize the effect of the differences of patients' anatomy.
- Comparing different sequences across one subject. For instance, we can have a T1w image of a patient and a T2w image of the same patient and we want to register them together. This allows comparing the sequences more easily and can give more informations about the patient.
- Registration also allows the construction of atlas. In medical imaging it can be of great interest to compare an image to a reference one, that is for instance non-pathological. This reference image is called an atlas, and to obtain it we usually combine many images from to different patients to obtain a kind of "mean image". Also, the reference image is usually of greater resolution, allowing to infer the position of details seen on the atlas but not on the image.
- Registration also allows us to register "real-time" image to other image. For instance, a patient can undergo an MRI scan (which is quite time-consuming) before an operation and when being operated, the surgeon can use a quicker imaging method like X-ray imaging or ultra-sound while doing the surgery. Then we can register in real time the X-ray or ultrasound image to the more detailed MRI acquired before the operation.

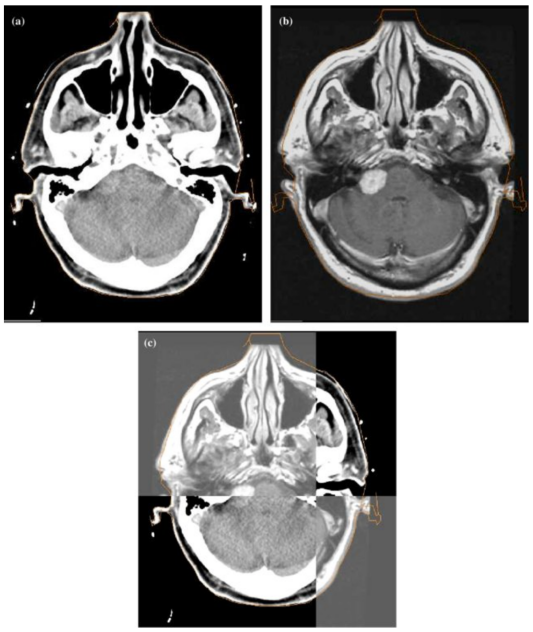

Figure 13: CT scan on the top left (X-ray), MRI scan on the top right, and superposition of the 2 images registered on the bottom [12]

2 Problem statement and state of the art methods

In this part we will first state the problem we are trying to solve, explain how it is "solved" right now in SCT and give some insight about registration methods and symmetry detection algorithms. Those elements will be useful later when explaining our contributions to the problem.

2.1 Problem statement

When registering two spinal cord MRI images, we wish to compute the transformation that allows us to map one image to the other (as we can see on the figure 14). To compute this transformation, multiple techniques can be used as we previously stated. The one we are interested in is the rigid transformation, which consists only of a translation and a rotation.

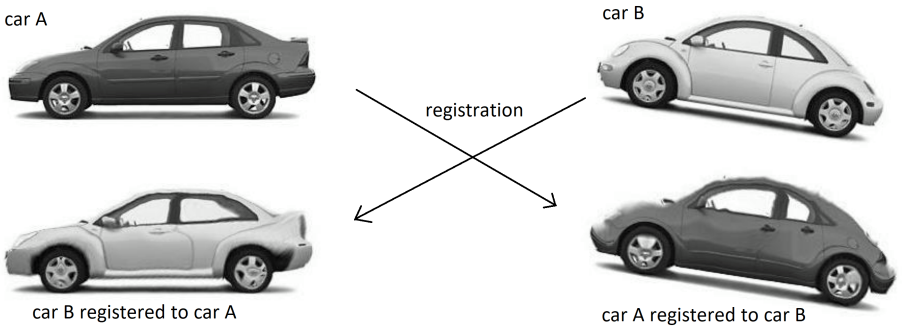

Figure 14: Figure illustrating the principle of registration [8]

Since our work focuses on the spinal cord, we can safely assume that there is almost no movement in the Inferior-Superior direction because the patient is lying down in the MRI scan, thus the problem will be to determine the rotation of the spinal cord in the transverse plane (figure 15 and 16).

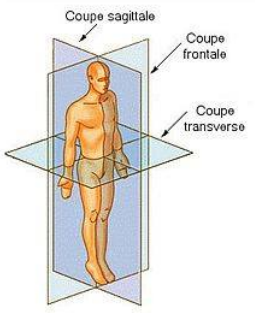

Figure 15: Schematic of the different plane names used in the medical field [29]

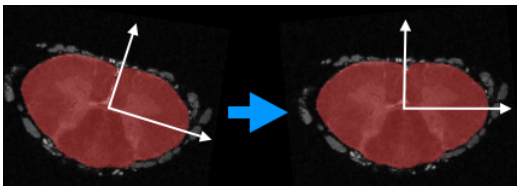

Figure 16: Simple schematic of the problem we wish to solve

Spinal cord rotation in the transverse plane can occur when the subject tilts its head while being in the scanner, an MRI of a rotated spinal cord can be seen on the figure on the main page.

This problem, which seem quite simple at first glance, can be tricky when dealing with low resolution images. The spinal cord diameter approximately ranges from 6.4 mm to 13 mm, which is quite small when dealing with image of resolution near 1 mm^3.

Once we have determined the angle of rotation of the spine on 2 different images, we will be able to compute the rotation that maps one to another.

Since the MRI image here is a 3D volume, we will need to compute the angle of rotation for all slices, but the task is, for now, done separately on each slice, thus making it a 2D image rotation detection problem.

To summarize, our problem is to detect the angle of rotation of the spinal cord in the transverse plane. To do that we will have access to the MRI image and the segmentation of the whole spinal cord[6].

2.2 Current method

Currently in SCT, a certain method is used to solve our problem. This method will be our direct challenger and the goal is to do better, that is, detecting more accurately and more robustly the rotation of the spinal cord, ultimately leading to a better registration.

The method is quite simple, and we will call it the PCA method. The method only uses the segmentation of the spinal cord, with one strong hypothesis : the spinal cord is ellipsoidal. We compute the PCA (Principle component analysis [39]) on the segmentation (which is a binary mask), this will output the two principle axis of the segmentation, wich will be, if the segmentation is ellipsoidal, the major and minor axis of the ellipse.The minor axis of the ellipse will give us the orientation of the spinal cord as we can see figure 17.

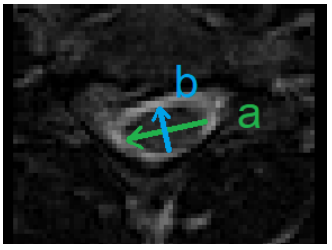

Figure 17: Major and minor axis of the ellipse superposed with the MRI of the spinal cord

This method has a major flaw : the strong hypothesis that the spinal cord is ellipsoidal can be in many case false (see for instance figure 18). Anytime the segmentation will not be close to ellipsoidal, the axis determined could be really far from reality.

[6]Because at that point in the registration pipeline, we have already segmented the spinal cord in the image

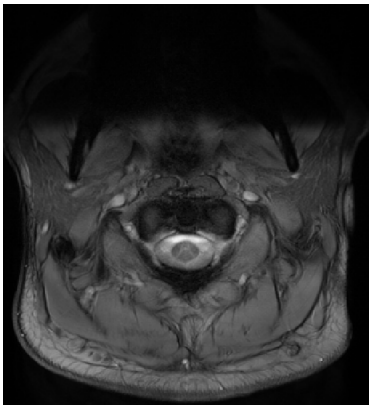

Figure 18: Example of an almost-round spinal cord

We wish to propose a method that is efficient and more importantly more robust to varying spinal cord shapes.

2.3 Registration methods

2.3.1 General context

We wish to give a little insight on the more global context of registration, even though our work is included in the simple case of rigid registration. This is also interesting because in SCT, more complex registrations methods will be used following the rigid registration

So far a handful of registration methods have been developed for medical images, a global review is done in [7].

We can define a more general mathematical formulation of the registration than before,

We define an image I as :

$$I : \boldsymbol{x} \mapsto I(\boldsymbol{x})$$
$$\Omega \to \mathbb{R}$$

With $\Omega \subseteq \mathbb{R}^d$, in our case $d = \{2, 3\}$ depending if the image is 2D or 3D. Meaning an image is a function that takes a position $\boldsymbol{x}$ (the pixel) included in a subset Ω (the image) and attributes it a value $I(\boldsymbol{x})$ (the pixel's value). Because images are quantified, in reality $\Omega \subseteq \mathbb{Z}^d$, but we will deal with quantification latter.

We define the correspondence map φ as :

$$\varphi : \boldsymbol{x} \mapsto \varphi(\boldsymbol{x})$$
$$\Omega \to \Omega$$

This means that the registered image will be $(I \circ \varphi)(\boldsymbol{x}) = I(\varphi(\boldsymbol{x}))$.

When registering an image I to another image J we want two things with the correspondence map :

- *Similarity* : to ensure the similarity between the destination image J and the registered image $I \circ \varphi$ we can calculate a dissimilarity metric Π between J and $I \circ \varphi$, meaning we will want to minimize $\Pi(I \circ \varphi\ ,\ J)$ as it gets bigger when the registration is not close enough to the expected result.
- *Regularity* (or smoothness) : to keep anatomical consistency we need φ to have a certain regularity, for instance belonging to $\mathcal{C}^1$, $\mathcal{C}^2$ or even more regular (this method is called implicit). One way to have this regularity in another way than to impose the regularity is to calculate a regularity metric (explicit method) like : $||L(\varphi)||$, where L is a differential operator, if the derivatives up to a certain order are not too big, this ensures the smoothness of the correspondence map.

Then, we want to minimize a sum of these two metrics (and thus compromise between similarity and regularity).

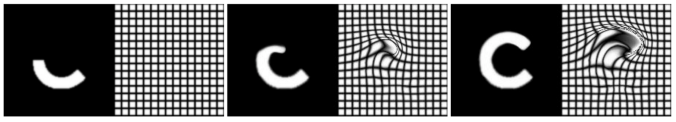

Figure 19: In each triplet, the left is an image and the right the associated warping field (correspondence map), the semi-C is being warp into a C [**?**]

In the simple case of rigid registration that we described before, φ is just an affine function : $\varphi(\boldsymbol{x}) = \mathbb{A}\boldsymbol{x} + \boldsymbol{b}$. This means in this case we use implicit regularity because the function we search for is by definition C^1.

Another property we wish to have for the correspondence map is the invertibility, if the map is invertible, this means we can use φ to register from one domain to another and also use φ^{-1} to do the registration the other way. This will allow more flexibility in comparing an image to an atlas for example. In other words, we want φ to be bijective.

In a certain way, there are two manners to compute the correspondence map :

1. Finding the parameters of the correspondence map directly by a certain method that is based on a priori knowledge, when doing this, the regularity is obtained implicitely by restraining the map search to a certain domain (for example linear registration) and the similarity is expected to be good because of the a priori knowledge that the method is "right" (but can be evaluated latter on to ensure this)
2. Finding the parameters by minimizing a cost function, that will try to optimize both the regularity and the similarity. This requires that the metric for similarity can be trusted, which sometimes is not trivial. We also need to search for the minimum with adequate method.

We can view the first method as a direct method and the second one as one with a "feedback loop".

Registration methods have been largely developed for the brain([13], [14], [8]), and are implemented in software that we have cited before. It is useful to look at brain registration method because as we have described in section 1.3, the spinal cord is in a way, similar to the brain because it is composed of the same tissues (i.e. white and grey matter, cerebro-spinal fluid), therefore we can try to adapt brain methods to the spinal cord or at least it can give us ideas to do so.

We will quickly describe a method that is used in SCT, described in [8] : the symmetric image normalization [8].

2.3.2 Study of an example: the SyN method

small and large deformation symmetric : same result regardless of the order of the inputs and invertible this method was tested for brain Which family of methods it is from which advantages how it works briefly

The SyN search the correspondence map φ to be a diffeomorphism, i.e. a smooth and invertible function. The basic principle is that velocity fields $v(\boldsymbol{x}, t)$ and $\phi(\boldsymbol{x}, t)$ are defined on Ω, with $t \in [0, 1]$. Here the correspondence map will be $\varphi = \phi(\boldsymbol{x}, 1)$ and $\phi(\boldsymbol{x}, 0) = \boldsymbol{Id}$ The velocity fields respect the following Eulerian-Lagrangian[7] equation :

$$\frac{d\phi(\boldsymbol{x}, t)}{dt} = v(\phi(\boldsymbol{x}, t), t)$$

[7]Here ϕ is in the Lagrangian frame and v is in the Eulerian frame. More details about the Eulerian and Lagrangian frame of reference in [30]

With this constraint on the velocity field, we will search to minimise the following term :

$$E(I,J) = \underset{\phi}{inf}\Big\{ \int_{t=0}^{1} ||L(v)||dt + \int_{\Omega} ||I(\phi(\boldsymbol{x},1)) - J||^2 d\Omega \Big\}$$

This will give us the correspondence map $\phi(\boldsymbol{x}, 1)$. We can see here as we have stated in section 2.3.1 that the minimization is opering on two different terms :

- A regularisation term on the velocity field v, applied by the differential operator L
- A similarity term, which is here a simple square difference of the registered image and the target image[8].

A neat addition is given in [8], the velocity fields are actually separated in two, for instance instead of computing Φ the authors will compute Φ_1 and Φ_2. Φ_1 will map I to a median image and Φ_2 will map J to a median image. This way the problem is being symmetrised and there is no difference in mapping I to J or J to I. An illustration is given on figure 20.

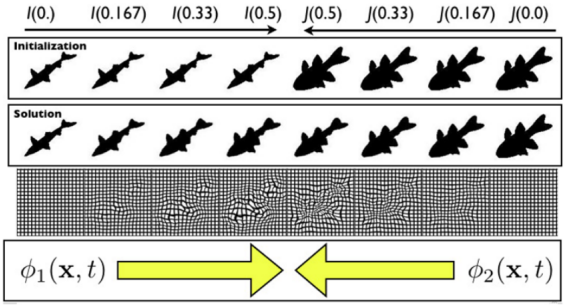

Figure 20: Two fish images are being registered one to another, we can see from top to bottom the initilisation, the last step and the warping field [8]

The main advantages of this methods are :

- The correspondence maps found are smooth and invertible due to the computation based on transport equations (we could say that the images are like fluids being moved one to another by a velocity field)

[8] A more complex metric than a square difference can be applied here, and that is what is done in [8]

- Different metrics (square difference, mututal information, cross-correlation, etc.) and differential operators can be used, thus the method is flexible
- By the symmetrisation of the optimisation, there is no difference between registering the source image to the target or the other way around
- Authors signal a similar computation cost compared to others similar diffeomorphism matching methods

More details about the overhall approach of diffeomorphism and velocity fields are given in [31]. We wanted to add that in their paper [8], the authors test their algorithm on brain MRI, like we said before, spinal cord MRI is a rare case of application and we will need to transpose brain MRI techniques to our problem.

2.3.3 Tools avaible in SCT

When doing a registration in SCT the available methods are :

- Translation (by centermass of the segmentation)
- Translation + rotation (by the PCA method)
- Affine transformation using ANTS [17]
- Syn method [8], which we presented before
- bspline syn method [15], which is a syn-like method but where the velocity field is computed as a composition of B-spline functions
- Slicereg method [16], which is a computation of the registration slice by slice but with a cost function defined over the whole spine, ensuring the regularity of the registration
- Scaling along the x axis and then segmentation border matching (non linear) along y (this method is advised for compressed spinal cord)

These different methods can be combined to allow more flexibility in the registration, for instance we can do translation + rotation as a first step and then a syn method to adjust for the smaller, non linear deformation.

In this report we are primarily interested in the simple rigid transformation : translation + rotation, because it is where our method is supposed to outperformed the PCA method.

As a rule of thumb, we can say that the simplest registration method allow for large transformation and should be applied first, and that non-linear more complex

methods are better used as a fine tuning. In general we also want the whole transformation to be invertible, which is always the case with linear transformation but in something we need to impose when searching for non-linear transformation.

2.4 Symmetry detection

As we will justify later , we are are interested in symmetry detection algorithms. To be more precise we are interested in reflectional symmetry (figure 21).

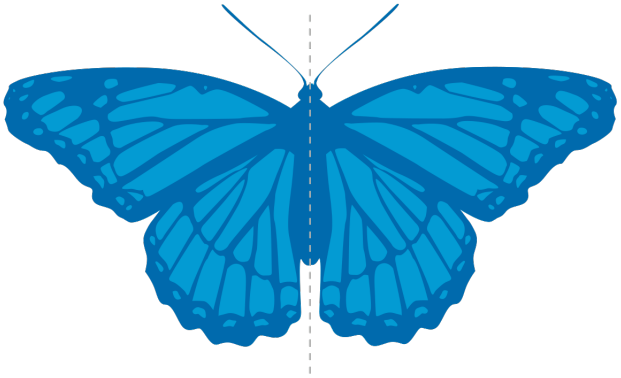

Figure 21: This image of a butterfly posses reflectionnal symmetry along the vertical axis [20]

Since we are not considering learning based approaches, there are two main family of reflectional symmetry detection algorithms :

- Feature-based algorithms : in these algorithms, first, we compute some features across the image, then try to infer the symmetry axis based on the position and the contents of the feature.
- "Pixel-wise" algorithm : in these algorithms, we try to infer the symmetry axis based on pixel information directly, we do not reduce the image to a smaller set of feature first[9].

[9]Actually, if we consider feature as small as one pixel, i.e. one feature per pixel, then we can say we do not differentiate the two categories

2.4.1 Feature-based algorithms

One way of detecting bilateral symmetry in images is to first extract features in the images, and then try to compute s symmetry axis based on thoses features.

In [**?**], Akbar and al. uses the well known scale-invariant feature transform (SIFT) [36] to gather features. They then evaluate the centroïd of all the feature points, and try to evaluate pair of pixels symmetric to the centroïd. The figure 22 is presenting an image with its SIFT feature points.

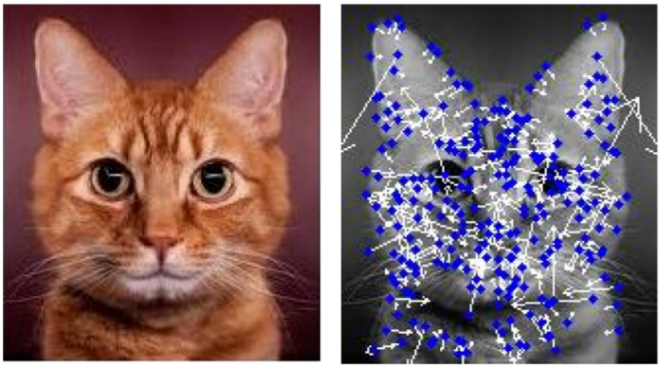

Figure 22: Image of a cat on the left and the associated SIFT feature points on the right [35]

To evaluate those pairs of pixels they compute the gradient magnitude and orientation on a small window around the two points and then compare the values obtained (as we can visualize figure 23), if they are similar the pair of points will vote proportionaly for the candidate line of symmetry. This goes on and on for each pair of candidate points, at the end the line of symmetry that has the more votes is the axis of symmetry detected.

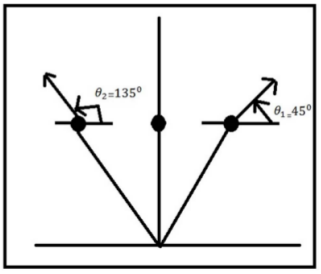

Figure 23: A pair of points being compared on the basis of their local gradient magnitude and gradient orientation [35]

The authors conclude that the method is efficient if only one major object is present in the image, multiple object will trick the algorithm.

In the paper by Loy et al. [32], the authors use any feature descriptor[10] (for instance SIFT) to gather feature points.
They then flip the image along candidate axis and re-compute the descriptor or if sufficient knowledge of the descriptor they flip directly the descriptor, e.g. if the descriptor is composed of only the orientation they flip the orientation.
The authors then compare the pair of points (the original point and the flipped one) and by a voting system, each pair of point will vote for its candidate symmetry axis, the vote being weighting by the similarity between the two points and other weighting such as distance from the middle point.
A figure showing the matching of pairs of feature points is showed in 24.

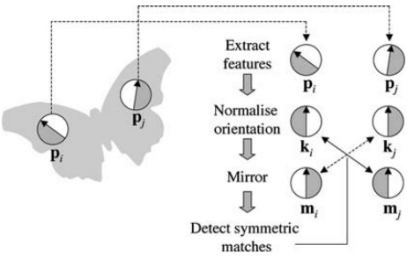

Figure 24: Pairs of points being matched to determine candidate symmetry axis [**?**]

The authors conclude that the method is efficient but highly dependent on the descriptor used. They also conclude that when image lack contrast, the small quantity of features points make the algorithm fail.

We will not focus anymore on these methods, the reasons why are given in the section 3.2.

2.4.2 Pixel-wise algorithm

What we mean by pixel-wise algoriths is a family of algorithms opposed to the ones based on features. Whereas feature based algorithms first group points together and then search for symmetry based on those groups, pixel-wise algorithms will try to search for symmetry directly with the information of all pixels, there will be no merging of points before the seek.

[10]The orientation being mandatory in the descriptor, and the more feature the better

A really basic and simple pixel-wise method being for instance, to try every axis of symmetry, and to compute the squared distance between the matching pixels from each side of the symmetry axis. This technique is rather basic but uses every pixels in the image.

Migalska et al. [37] use a simple reflection of the image like we described before(that is showed figure 25), but instead of computing a simple square distance between the image and its folded counterpart, they compute the Negentropy [**?**], a concept pioneered by Erwind Schrödinger.

Figure 25: Here we can the two halves of an image being reflected on on another [37]

This method can actually be generalized to many types of similarity measure, wheter be it square distance, Negentropy, Mutual information, cross-correlation, etc.[11]

The main paper we will be focusing on is the one by Sun et al. [3] which is an improvement of their previous paper [11].

The method described by Sun et al. is based on the orientation of the gradient. To obtain it they compute the x and y gradient (G_x and G_y) of the image I, i.e. :

$$G_x = \frac{\partial I}{\partial x} \quad \text{and} \quad G_y = \frac{\partial I}{\partial y}$$

We can then compute the gradient magnitude G_M and the gradient orientation G_θ :

$$G_M = \sqrt{G_x^2 + G_y^2} \quad \text{and} \quad G_\theta = \arctan(\frac{G_y}{G_x})$$

Note that $G_M \in [0, +\infty[$ and $G_\theta \in [-\pi, \pi[$.

In their two papers Sun et al. did only use the information contained in G_θ and not in G_M.

[11] More about entropy and mutual information in [38]

After that they compute the histogram $h(\theta)$ of G_θ, choosing a certain number of bins (for instance 360, one for each angle degree) which is a parameter. This parameter can be tuned as a function of the resolution, the more the pixels in the image the less the statistical dispersion into the many bins. $h(\theta)$ being a function of angle is obviously 2π periodic.

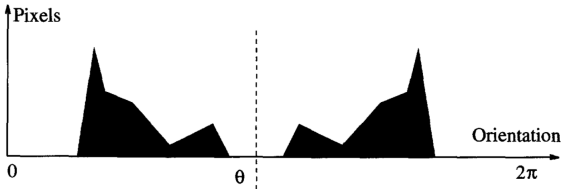

Figure 26: Example of an histogram of the gradient orientation, the number of pixels of certain angle is counted in y as a function of angle in x [11]

We can visualize an example of an orientation histogram on figure 26. It can then be observed that for an image possessing a bilateral axis of symmetry of angle α, the histogram of the gradient orientation will also be symmetric[12] along a vertical line at angle α meaning that because $h(\theta)$ is 2π periodic, we will have :

$$h(\alpha - \theta) = h(\alpha + \theta)$$

To search for the axis of symmetry we have to find the angle α verifying the former equality. To do that we can compute the the circular auto-convolution of $h(\theta)$:

$$(h \circledast h)(\theta) = \int_{-\pi}^{\pi} h(\theta - t)h(t)dt$$

Circular here means that because $h(\theta)$ is periodic we will limit the convolution to one period. The auto-convolution will show us where $h(\theta)$ best folds itself along a certain axis, meaning we can retrieve the angle of symmetry α by searching for the maximum of the autoconvolution :

$$\alpha = \frac{1}{2} \arg\max_{\theta}(h \circledast h)(\theta)$$

[12]The symmetry of the histogram for a symmetric image is guaranted but there can be symmetry in the histogram without a bilateral symmetry in the image, i.e. symmetry in the image $\Rightarrow$ symmetry of the histogram. This will not bother us because one of our assumption is that it exists a bilateral symmetry in the image.

The factor $\frac{1}{2}$ can be viewed as due to the fact that we search the axis of symmetry $\alpha \in [-\frac{\pi}{2}, \frac{\pi}{2}[$ because the axis is not oriented.
If there exist n axis of symmetry, one can search for the n^{th} maxima in the auto-convolution to retrieve all the axis.

In their second paper [3], Sun et al. improved the method by simply computing the auto-convolution using the Fourier domain to improve the computation speed. They did also add a fitting of a quadratic parabola to the maximum location, in order to detect sub-angular symmetry axis.
They also precised that if it exist a strong periodic pattern along a non-symmetry axis direction, the first maximum detected could not be the symmetry axis. This will not bother us because there is no periodic pattern (at least no strong one and not near the spine) in spinal cord MRI.
Here we have described everything with continuous mathematic tools but the images are discrete, we will adress later the problems of digitization.

To summarize, the method of Sun et al., although quite simple, allows for a fast detection of the principle axis of symmetry (or more) of the image.

3 Contributions

Now that we have exposed the global frame of our work, exposed the problem we are trying to solve, the current method used and gave some explanations about registration and symmetry detection algorithms, we will first give the reason and logic behind our choices before diving into the main contributions.

3.1 List of a prioris to the problem

We wish to give a clear list of all the *a prioris* we have with our problem. This will allow us to choose methods that fit best our needs, to modify algorithms to fit our problem and this will allow external readers to clearly see (and maybe corrects) our assumptions about the problem, which might be naive given our limited knowledge in the anatomy of the spinal cord.

- The spinal cord, in the transverse plane exhibits an anterior-posterior symmetry. When we say the spinal cord, we mean the spinal cord and the near environment of the spine.

- The anterior-posterior symmetry of the spinal cord gives us the angle of rotation.
- The angle of rotation should be relatively small, it is not anatomically possible to have a very large rotation if the patient has no serious lesion
- The rotation should be greater near the cervix than in the lumbar area, because it is the tilting of the head that leads to the spinal cord rotation
- Angles as a function of the superior-inferior axis are expected to have a certain degree of regularity if once again there is no serious lesion

We wish to say that we are not entirely satisfied with some of the asumptions we are making. The fact that the spine of the patient is expected to have a certain regularity exclude case where the patient could have a serious lesion. In the perfect scenario this *a priori* should not be used, but it improves greatly the method when used, and the lesioned patients represent a really small fraction of the cases, where the clinician could correct the angle manually.

3.2 Rationale justifying our approach

With the assumptions made in section 3.1, we can see that it is possible to use symmetry detection algorithms to try to solve our problem, hence our focus in section 2.4 on these types of algorithms. The PCA method was already using the segmentation to determine the orientation so we wanted not only to test another method but also to add information by looking at the image.

We want to remind the reader that at this stage we have access to the MRI of the spinal cord and its segmentation, as we can see figure 27.

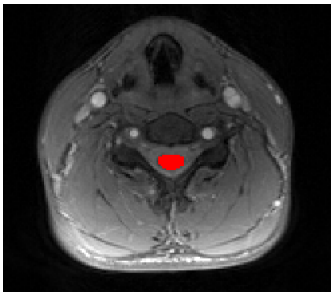

Figure 27: MTon sequence of spinal cord MRI with segmentation superposed in red

After reading about all the different methods presented in section 2.4, we decided

to try to adapt the method of Sun et al. [3] to our problem. The reason behind the choice of this method were :

- Simplicity : because we have quite a low resolution in our images, we consider that it is unlikely that a very complex method (usually requiring more information) will work, thus we tried a method which seems to work on low resolution images[13]. We will move on to a more complex method if we do not obtain sufficient results with this one.
- Not feature-based : the features we can find around the spinal cord can very much vary with the level of the vertebrae considered and from one subject to another thus it appears not to be a good choice to pick a method based on feature matching. Also, when registering images with different contrasts, it is possible that a feature visible on a certain image is not on another (for instance inflammation are visible on T2w but not on T1).
- Not learning based : we believe that our simple problem should have a "simple" solution, simple in a way that we can understand it and not treat it as a black box, considering that we will orient our research on non-learning based approach, using our a priori knowledge to build the best algorithm.
  Furthermore, if we wanted to train, for instance, a neural network, we would have to have proper ground truth, which we don't have, or use unsupervised learning approaches, which is a path we wish not to explore. Also, as we have said before, there is many contrasts and many vertebral levels in our images, meaning we will have statistical dispersion if we separate every contrasts and/or vertebral level, or poor robustness if we do not.

For now, this means we will only deal with transverse MRI of the spinal cord, this means our problem is a problem of 2D symmetry detection.

3.3 Proof of concept

3.3.1 Mathematical example

In this section, we will demonstrate how the method works on a continuous case, and on a simple image. We shall mathematically demonstrate that we obtain the axis of symmetry in the image by this method. We will apply the method of Sun et Si. [3] to the image presented figure 28.

[13]Thus, "old" methods, developped in the time where the images were not of really high resolution are very interesting for our problem

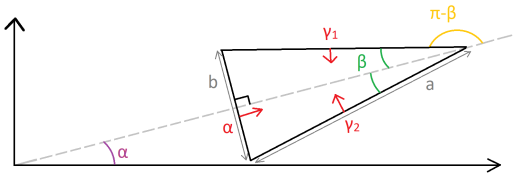

Figure 28: Continuous image of an isosceles triangle with an obvious axis of symmetry (line of angle α), the horizontal and vertical axis are not part of the image

At first, we need to calculate the gradient orientation histogram. We can clearly see on the picture that there are only 3 edges, one with length b and orientation α, and two with length a and orientation γ_1 and γ_2. By convention we will state that the gradient are oriented on the inside of the triangle, which corresponds to a white triangle on a black background (going the opposite convention will not change anything). We can quickly see that $\gamma_1 = \alpha - \beta - \frac{\pi}{2}$ and $\gamma_2 = \alpha + \beta + \frac{\pi}{2}$.

Since the histogram is 2π periodic (because counting for angles), we will draw it in a circular fashion, for easier visualisation :

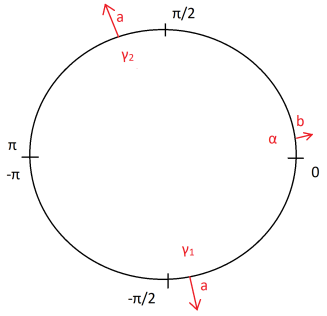

Figure 29: Orientation histogram of the image 28

Since the image is continuous[14], we will take the limit of the histogram as the number of bins approach 0. If we note $h(x)$ the histogram graph function, h is :

$$h(x) = b\mathrm{III}_{2\pi}(x-\alpha) + a\mathrm{III}_{2\pi}(x-\alpha-\beta-\frac{\pi}{2}) + a\mathrm{III}_{2\pi}(x-\alpha+\beta+\frac{\pi}{2}) \quad \text{for} \quad x \in \mathbb{R}$$

With $\mathrm{III}_T(x-x_0) = \sum_{k=-\infty}^{\infty} \delta(t-kT-x_0)$ the Dirac comb function centered in x_0 and T periodic.

[14]There is infinitely many "pixels" in a certain way, for each edge

Because we deal with periodic functions, we define the circular convolution between two T periodic functions h_1 and h_2 as :

$$(h_1 \circledast h_2)(x) = \int_{-T/2}^{T/2} h_1(x-t)h_2(t)dt$$

We can demonstrate that :

$$\mathrm{III}_T(x-x_1) \circledast \mathrm{III}_T(x-x_2) = \mathrm{III}_T(x-x_1-x_2)$$

With this property we can calculate the circular auto-convolution of the histogram :

$$\begin{aligned}(h \circledast h)(x) = {} & b^2\mathrm{III}_{2\pi}(x-\alpha) \circledast \mathrm{III}_{2\pi}(x-\alpha) + a^2\mathrm{III}_{2\pi}(x-\alpha-\beta-\frac{\pi}{2}) \circledast \mathrm{III}_{2\pi}(x-\alpha-\beta-\frac{\pi}{2}) \\ & + a^2\mathrm{III}_{2\pi}(x-\alpha+\beta+\frac{\pi}{2}) \circledast \mathrm{III}_{2\pi}(x-\alpha+\beta+\frac{\pi}{2}) \\ & + 2ab\mathrm{III}_{2\pi}(x-\alpha) \circledast \mathrm{III}_{2\pi}(x-\alpha-\beta-\frac{\pi}{2}) \\ & + 2ab\mathrm{III}_{2\pi}(x-\alpha) \circledast \mathrm{III}_{2\pi}(x-\alpha+\beta+\frac{\pi}{2}) \\ & + 2a^2\mathrm{III}_{2\pi}(x-\alpha-\beta-\frac{\pi}{2}) \circledast \mathrm{III}_{2\pi}(x-\alpha+\beta+\frac{\pi}{2})\end{aligned}$$

Meaning we have :

$$\begin{aligned}(h \circledast h)(x) = {} & (a^2+b^2)\mathrm{III}_{2\pi}(x-2\alpha) + a^2\mathrm{III}_{2\pi}(x-2\alpha-2\beta-\pi) + a^2\mathrm{III}_{2\pi}(x-2\alpha+2\beta+\pi) \\ & + 2ab\mathrm{III}_{2\pi}(x-2\alpha-\beta-\frac{\pi}{2}) + 2ab\mathrm{III}_{2\pi}(x-2\alpha+\beta+\frac{\pi}{2})\end{aligned}$$

We have $\theta = \frac{1}{2}\arg\max_x (h \circledast h)(x)$ the angle of symmetry of the image.

And since $a^2+b^2 \geq 2ab$ and $a^2+b^2 \geq a^2$ we can see that the maximum of $(h \circledast h)(x)$ is at $x = 2\alpha$, meaning we have $\theta = \alpha$. This result can be seen easily, the axis of symmetry on the figure 28 is clearly the line of angle α.

Note for part 3.3.2 that $h(x)$ have 3 peaks and $(h \circledast h)(x)$ have 5.

With this example, we have gone trough the whole process of determining the axis of symmetry on an image, as a proof of concept. In reality, this will go a little bit different because of the quantification of the image (image is a $\Omega \subset \mathbb{Z} \to \mathbb{R}$ function rather than $\Omega \subset \mathbb{R} \to \mathbb{R}$). We will have to take care of digitization effects.

3.3.2 Simple images case

First of all, we tried to implement the method of Sun et al. [3] and test it on basic images, to be sure that the method works on simple cases (images with obvious axis of symmetry) before testing in on real data.

There is quite a few thing that we need to precise in dealing we the quantification :

- We compute the gradient orientation as $\arctan(\frac{G_y}{G_x})$ with G_x and G_y respectively the x and y gradient [15]
- When computing the histogram we had to choose a number of bins, we chose 360 (one per angle degree) but this is a parameter we can modify if we want
- When smoothing the histogram, we use a certain filter, but the order and the type of the filter are also a parameters (we used a median filter like in [3] and we chose 3 for the order, this is also a modifiable parameter)
- When searching for the maximum, we used a simple function that compares the value with its n neighbours to define if it is a maximum or not, n is also a parameter (we chose the same as the order of the median filter, 3)

First we show the results of the method on an image similar from the part 3.3.1, the image on the figure 30, the image is blurred to avoid at best digitization effects that we will explain latter.

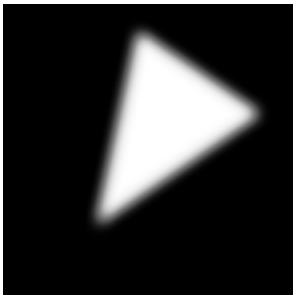

Figure 30: Image of a blurred triangle, similar to the theoretical example on figure 28 with axis of symmetry at 34 degrees

We then compute the gradient orientation histogram (GOH), smooth it and compute the auto-convolution :

[15] Precisely we use the *atan*2 function [21] which maps to $[-\pi, \pi[$ instead of $[-\frac{\pi}{2}, \frac{\pi}{2}[$ for *atan* to compute exactly the orientation of the gradient

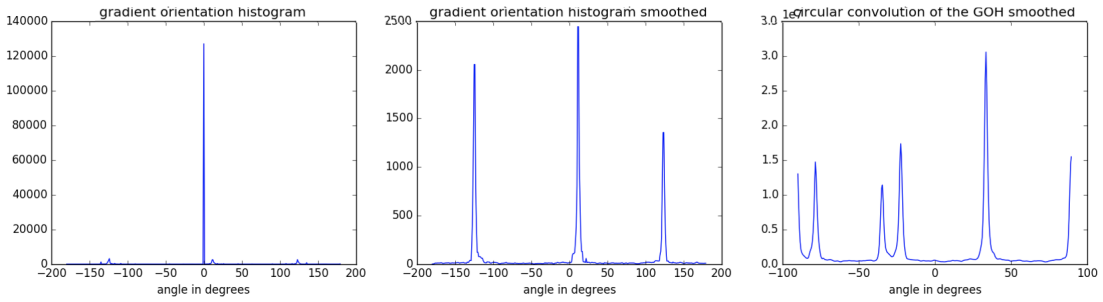

Figure 31: GOH, smoothed GOH and auto-convolution of GOH of the figure 30

Just like we predicted in the part 3.3.1, we can see 3 peaks on the (smoothed) histogram, because there is 3 sides to the triangle. After auto-convoluting the histogram we obtain, like we predicted, 5 peaks, with a maximum at angle 34, giving us the axis of symmetry of the image. We can visualise on figure 32 the axis drawn.

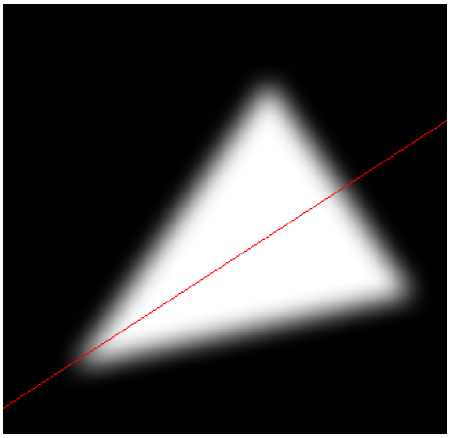

Figure 32: Figure 30 with the axis found drawn on it in red

Note here the importance of the smoothing step, leading to the expected result. We will give an example showing the utility of the smoothing :

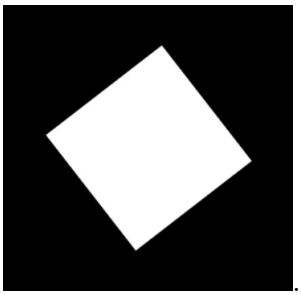

Figure 33: Image of a squared rotated by 52 degrees

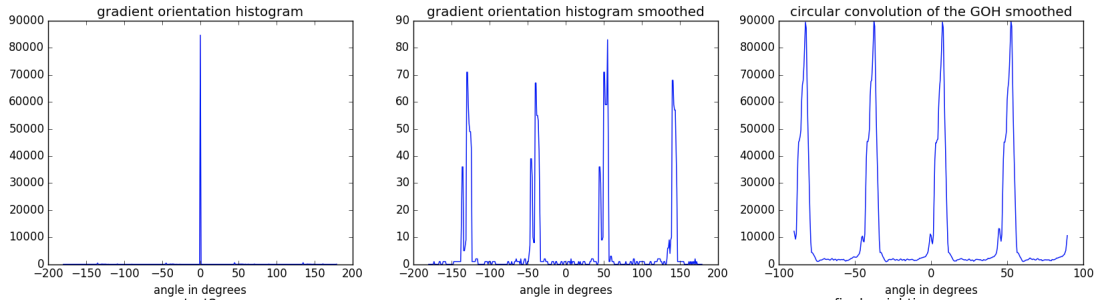

Figure 34: GOH, smoothed GOH and auto-convolution of GOH of the figure 33

Here the square is not blurred at all, unlike the previous image. What happens in the images is that because of digitization, the boundary of an object consists mostly of zigzagged short line segments, and very often these line segments are either horizontal or vertical with diagonal segments connecting the horizontal or vertical short lines. Therefore, in most of the gradient orientation histograms, peaks often appear at 45° and multiples of 45° (such as 0°, 90°, 135°, -45°, etc.).

We can clearly see this effect for this image, which is supposed to only have orientation of 52°, 52 +90°, 52 -90° and 52 - 180° (the "big" peaks, the smaller ones being the "45°" ones).

The smoothing is supposed to reduce those peaks effects near multiple of 45°, but even with the smoothing we can still see on the figures this effect. We partly address this effect in section 3.4.

This effect is also more prominent on image with better resolution, the more the resolution, the more there are small segments "voting" for angles multiples of 45°, meaning we will need to adapt the smoothing with the resolution.

Apart from that, we can still view that the method finds the angles of symmetry of

the image, 52, 52+45 (the diagonal of the square), 52 + 90 and 52 - 45 (the other diagonal).

For now we have shown that the method allows to find the one or multiple axis of symmetry of the image, but we also wish to show that with an image that has no symmetry, we don't find axis of symmetry :

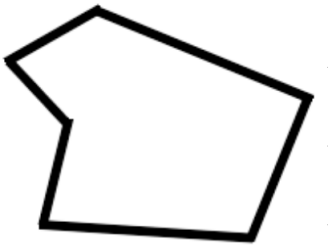

Figure 35: Image presenting no axis of symmetry

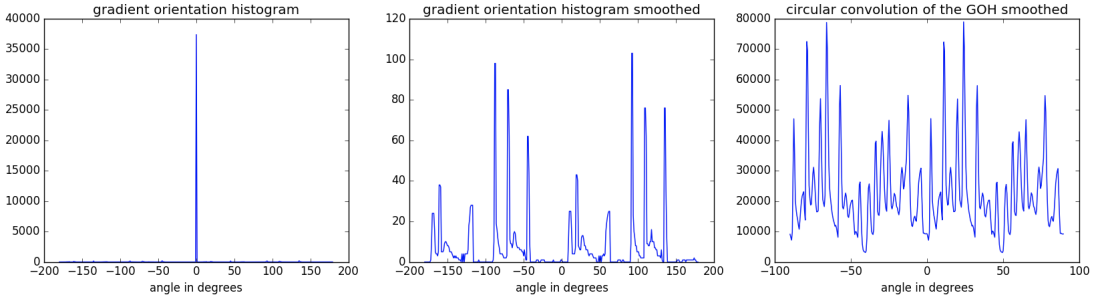

Figure 36: GOH, smoothed GOH and auto-convolution of GOH of the figure 35

As we can see on the right of the figure 36, there is clearly no clear maxima like on the previous figures, the circular convolution of the histogram is "messy" and we cannot get a proper symmetry axis. This means that with an appropriate criterion on determining if the maximum is "a true maximum"[16] we should be able to determine if the symmetry detected is indeed a "true symmetry".

3.4 Adaptation to the problem and improvements

After showing that the method works on simple images, we wish to adapt the method to our problem and if possible to improve it. The goal here is to determine the angle

[16]For instance by computing $\frac{max_1}{max_2}$ or $\frac{max_1}{mean}$

of rotation of the spinal cord. Under the assumptions made in the beginning of part 3.1, we will find this angle by detecting the symmetry present in a transverse spinal cord MRI.

The two main improvements of the method of Sun et al. [3] that we will describe have the same key concept : weighting the gradient orientation histogram. That is something the authors did not do in their paper and which we haven't found in the literature. It is a simple but efficient concept : each pixel on the image will not have the same impact when voting for the orientation in the histogram.[17]

A typical spinal cord transverse MRI looks like figure 37, as we can see, the spinal cord only represent a small portion of the image, meaning there will be many features that will contribute to the voting on the histogram but that are not part of the spinal cord.

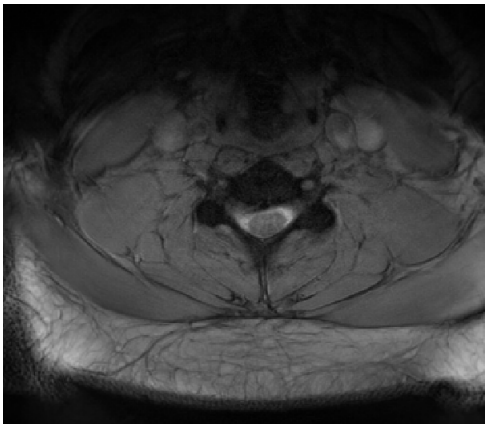

Figure 37: T2* MRI slice at the cervical level

3.4.1 Weighting by the distance to the centerline

We can also see on the figure that the spinal cord is rotated, the neighbourhood of the spinal cord seems a little bit rotated but the structures that are far from the spinal cord are not rotated at all, meaning the region of interest is only near the spinal cord. Also, this rotation from the nearest structures is done in a continuous fashion : tissues extremely close to the spine are extremely rotated, tissues somewhat close to the spine are somewhat rotated, and so on. This point wil

To deal with this issue, our first improvement/adaption from the method of the method of Sun et al. [3] is the following :

[17] We had this idea of influencing the vote because it is exactly what is done in the algorithms that improve Hough transform method, which something I had personally worked on before

Because at this step we have the whole spinal cord segmentation[18] we will weight the histogram by a score related to the proximity of the spinal cord, in this way, the structure close to the spinal cord's vote will count more than those which are far from it. To do that we weight the image by a Gaussian function[19] centered at the barycenter of the segmentation and which standard deviation depends on the pixel dimension[20]. The maps obtained looks like figure 40.

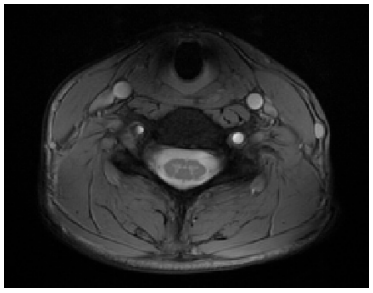

Figure 38: T2* MRI slice at the cervical level

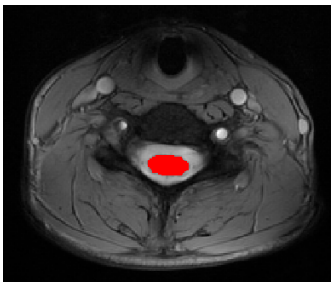

Figure 39: Same MRI slice with segmentation of the spinal cord superposed in red

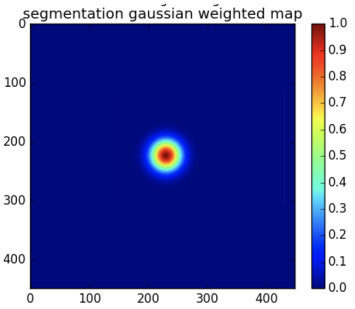

Figure 40: Gaussian weighting map coming from barycenter of the segmentation

With this adjustment, we can account for the vote *gradually* from the structure that are close to the spinal cord. On figure 40, the importance of the vote is accounted by a score between 0 and 1.

3.4.2 Weighting by the gradient magnitude

Our second improvement to the method of Sun et al. is again, a weighting of the histogram. In their original paper Sun et al. did not account for this : when computing the orientation gradient, every pixel will output a value, an orientation, whether or not it has an actual significant orientation. Even, at the end of their paper [11], they declare that "The magnitude of the gradient has not been used".

[18]To display the axis of symmetry we will use the angle computed by our method and the barycenter of the segmentation to draw the line

[19]It is necessary to have a gradual voting importance, if we take only into account the vote of the pixels in the segmentation, we risk the same problem as with the PCA method presented in 2.3 if we don't see the interior butterfly shape of the spinal cord

[20]Say that the vote from only the pixels that are distant from 20 pixels of the barycenter count, in one image 20 pixels could be equivalent to 20 mm and in another one 10 mm, to nullify this effect we need to normalize by the pixel dimension

It is rather clear that it is the pixels from the edge that determine the orientation of the structure, the orientation of pixels on regions which are homogeneous will be mainly decided by the noise of this homogeneous structure, which is quite random. Our idea was to weight the gradient orientation histogram by the magnitude of the gradient. This way only the pixels that have a strong orientation will vote, and vote from pixels in homogeneous region will not count as much.

To test this second idea, we tried to apply this improvement to simple images :

Figure 41: Test image of a mask, rotated by -30 degrees

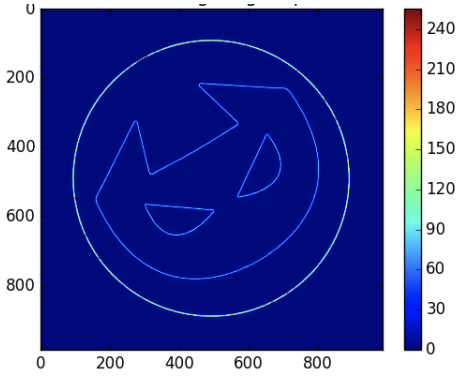

Figure 42: Gradient magnitude of the mask, used as a weighting map[1]

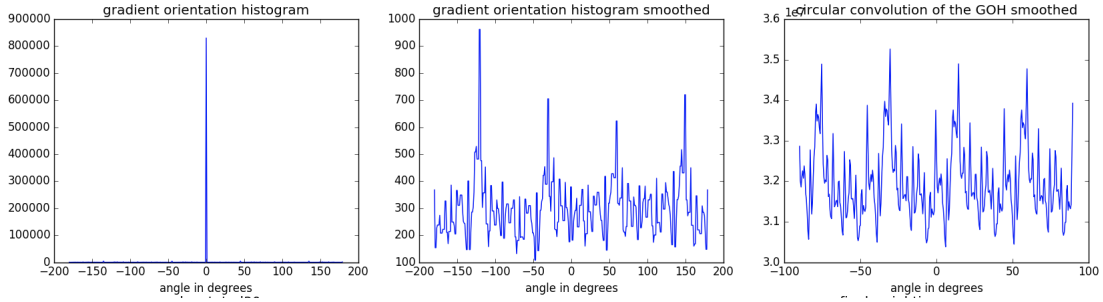

Figure 43: GOH, smoothed GOH and auto-convolution of GOH of the figure 41 with no weighting by the gradient magnitude

[1]The gradient magnitude map has been normalised here between 0 and 255 just for display

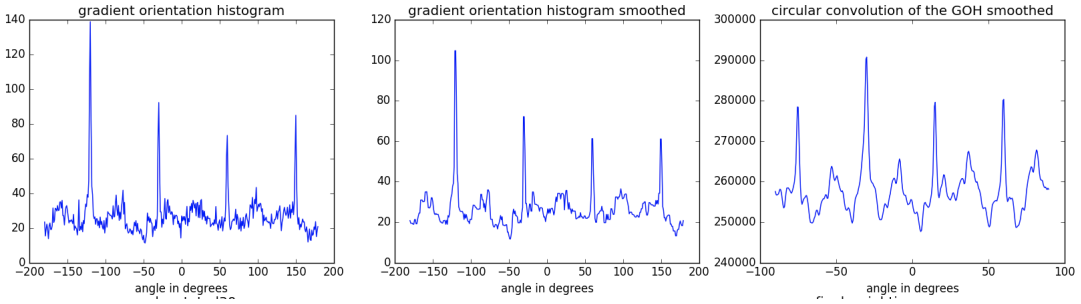

Figure 44: GOH, smoothed GOH and auto-convolution of GOH of the figure 41 with weighting by the gradient magnitude

As one can notice from the figure 43 and 44, the addition of the weighting map by the gradient magnitude effectively reduce noise in the GOH and in the end in the circular convolution of the GOH. This allows clearer demarcation of the maximum and thus improve the *robustness* of the method.

This noise reduction address in a certain way the "45° problem" raised in section 3.3.1, because by reducing the number of pixels that vote we reduce the number of votes for the "45°" angles.

3.4.3 Combination of the weighting and result

To summarize, instead of computing the gradient orientation histogram like Sun et al., we will compute a weighted gradient histogram, with weight map being a combination of a segmentation-based Gaussian map and a gradient magnitude-based map. The final weighting map for figure 38 is presented figure 45, this map makes a lot of sens because we can see that only the spinal cord and the structure around are taken into account and also it is the edges that import when voting and that is something wee see on this map. We can also assess the angle detected on figure 46 which seems quite accurate.

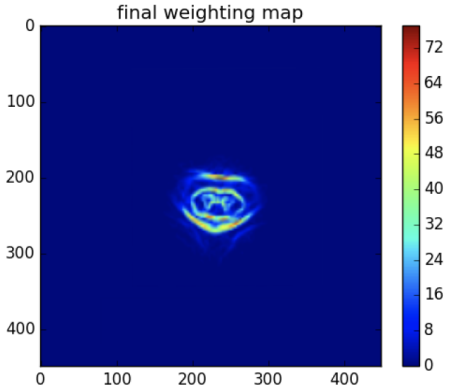

Figure 45: Final weighting map for the figure 38, combination of a Gaussian segmentation-based map and a gradient magnitude map

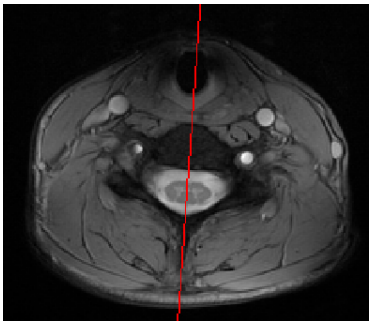

Figure 46: T2* slice of the figure 38 with the axis of 4° detected by our method in red

We can also visualize the associated GOH, smoothed GOH and auto-convolution of this image on the figure 47. The figure show a clear maximum at the position -86° (corresponding to a +4° angle, if the zero angle is considered north of the image).

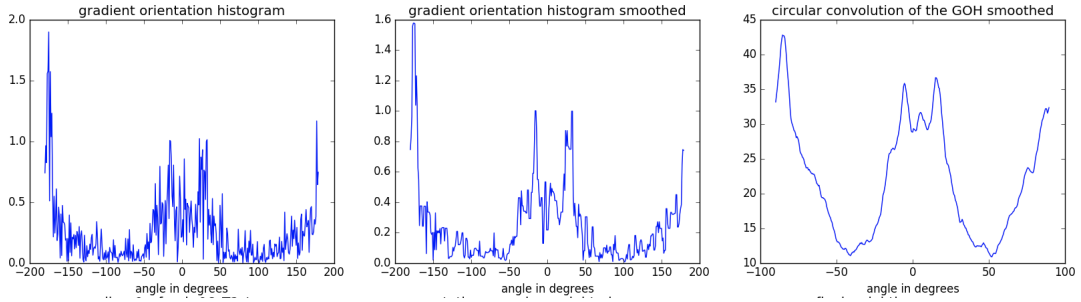

Figure 47: GOH, smoothed GOH and auto-convolution of GOH of the figure 38 with our method

In comparison, we can visualise the GOH, smoothed GOH and auto-convolution with the basic method of Sun et al., without our improvements in figure 48. It is rather clear that the final product is a lot noisier and that by our work we improved the method of Sun et al.

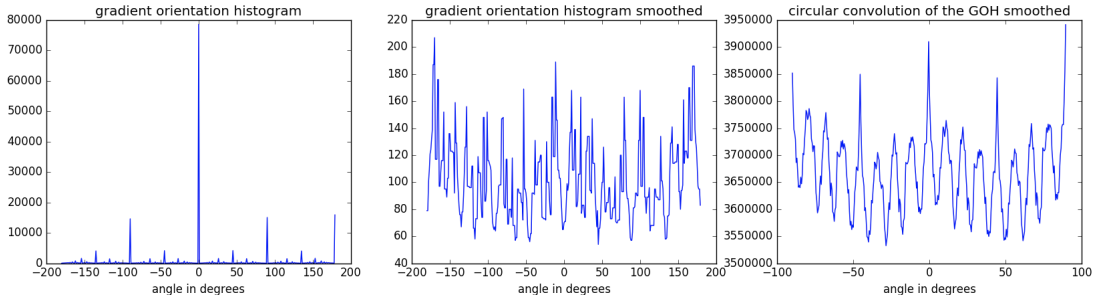

Figure 48: GOH, smoothed GOH and auto-convolution of GOH of the figure 38 with the "vanilla" method of Sun et al.

To summarize, our method goes like this for detecting the axis of symmetry in a spinal cord MRI[22] :

- Compute x and y gradient of the image[23]
- Use it to compute the orientation of the gradient and the magnitude of the gradient
- Use the barycenter of the segmentation to define a Gaussian segmentation weighting map
- Multiply the latter by the magnitude of the gradient to obtain the final weighting map (normalize both before doing so)
- Compute the histogram of the gradient orientation, each pixel's vote being weighted by the weighting map
- Compute the auto-convolution of the histogram
- Search for the maximum (and divide by 2) to obtain the principle axis of symmetry

3.4.4 Combination of old and new method

In the course of our work[24], we noticed that our method did not always outperform the PCA method. Instead of trying to build a whole new method which is supposed to outperform the older, we thought of combining the two methods together.

[22] Actually our method can be applied to any image where we already have the segmentation of the structure of interest

[23] The image can be normalized by its median before that, because the gradient magnitude computation is sensitive to constant multiplicative noise (which is frequent in MRI)

[24] As we discuss a little bit in the further section 3.6

To achieve this in an efficient way, we need to know when each method is certain about its result and when its not. If said method is unsure about its result, we can switch to the other.

We thought of introducing confidence score for each method, indicating the level of confidence/certainity that each method has about its result.

For the PCA method, the confidence score is the following :

Confidence score PCA method :
The complement of the ratio between the minor axis b and the major axis a determined by the PCA : $1 - \frac{b}{a}$

This is justified by the fact that the PCA method fails when confronted to quasi-round spinal cord. This will arrive when the segmentation is quasi-round, meaning the length of the axis a and b will be really close, this will lead to a confidence score close to 0.

For our method, the confidence score can be :

Confidence score 1 :
The ratio between the maximum found in the auto-convolution and the mean of the auto-convolution: $\dfrac{(h \circledast h)(\alpha)}{\sum_{\theta}(h \circledast h)(\theta)}$

This is the ratio between the maximum found and the mean of the signal, which indicate if the maximum is really prominent in the signal (here the auto-convolution). It will fail to detect when the second maximum is a good candidate too.

Or it can be the following :

Confidence score 2 :
The ratio between the 2 first maximum found (corresponding to angle α_1 *and* $\alpha 2$*) in the auto-convolution :* $\dfrac{(h \circledast h)(\alpha_1)}{(h \circledast h)(\alpha_2)}$

This will give a strong score when the axis detected is the only candidate for the symmetry. It will fail to detect when the signal possess almost no maxima.

When trying to conduct tests to see the relevance of the confidence score for our method, we did not conclude to good correlation between the validity of the angle detected and the confidence score, wheter be it the 1st or the 2nd. There was many "aberant"[25] angles that had either weak or strong confidence scores and "reasonable"

[25]It is difficult to evaluate precisely at 1^o or 2^o the validity of a symmetry axis but it is sometimes

angles that had either weak or strong confidence scores. We did not include these confidence scores in our final work, but we believe it is a path worth searching for.

On the other hand, the PCA confidence score did show good result. The symmetry axis detected when the spinal cord was quasi-round were almost random, where the axis detected when the spinal cord was ellipsoïdal were really often 'reasonable".

We decided to use the PCA confidence score to build an "automatic" method.

1. Compute PCA to determine minor and major axis
2. If PCA confidence score is high enough, stop here and take for angle of symmetry the one determined by the minor axis
3. If PCA confidence score is too low, output the angle determined by our method

We added also a prioris on the results we expect, for instance it is really unlikely that we will have angle outside the range $[-20, 20]$ degrees (this is a parameter we can change), thus we will abandon PCA results that are outside this range and for our method we will search the maximum only in the said range.

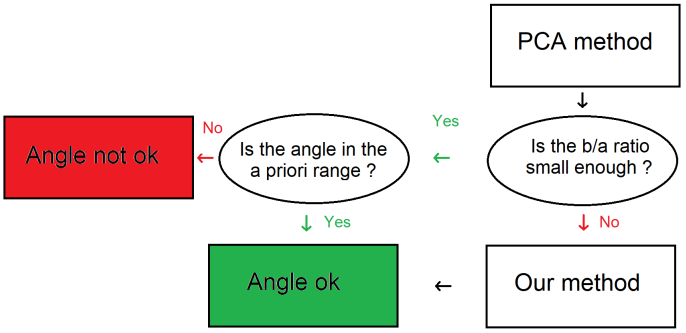

Figure 49: Block diagram of the automatic method

This method as we will demonstrate later, did show better result than PCA alone and our method alone.

3.5 Evaluation method

For now, we have seen by looking at the histogram that our method seems better than Sun et al.'s method because it seems less noisy. We have also shown that the axis determined are visually pleasing.

really easy and sure when the difference is really big.

However, if we wish to assess the real improvement of our method, we need a real qualitative and quantitative assessment. This way we can compare in a much more robust way with the PCA method (and the Sun et al. vanilla method if we wish to).

For a reminder, we want to know if the angle detected for the rotation is "the good angle". This task which seems simple is actually really not trivial because :

- We do not know the real angle (we have no ground truth, no labels on our data)
- We do not have the time and ressources (trained radiologists) to manually label a lot of images, which would provide a gold standard[26].

That being said we must find a way of evaluating our method without having the ground truth or professional radiologists at our disposal.

We will propose different ways of evaluating our method, none being perfect but each one complementing each other, that match our ressources.

For a reminder, we need to find the angle of rotation based on the spinal cord MRI and its segmentation. We will compute the centroïd of the segmentation to have one point by which the symmetry axis will pass and retrieve the angle with our different methods.

3.5.1 Qualitative evaluation

To conduct a qualitative evaluation, we must see and compare the effect of our method VS the PCA method. We propose a visual check on a great number of 2D MRI slices to asses our method, and maybe try to understand in which case it goes wrong and try correcting it.

We propose 2 different kinds of visual checks :

1. Visually checking the axis of symmetry detected by superposing the axis to the image.
2. Visually checking the rigid registration (translation + rotation) by alternatively viewing source image registered and target image

Those two methods can seem redundant one to another but it gives two different perspectives on the same result and allows complementary evaluation.

[26]To be really accurate we would also need to have multiple radiologists labelling the data

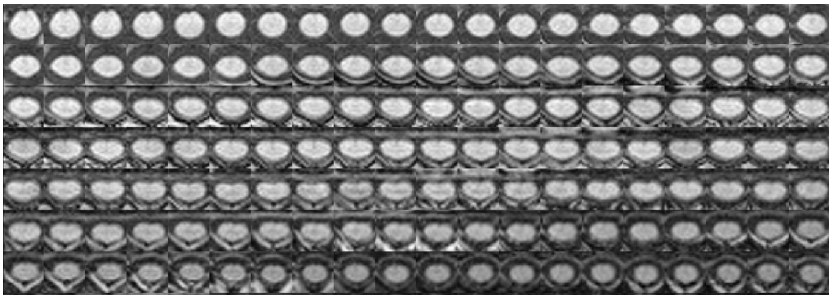

Figure 50: Quality control (visual control) of the source image registered

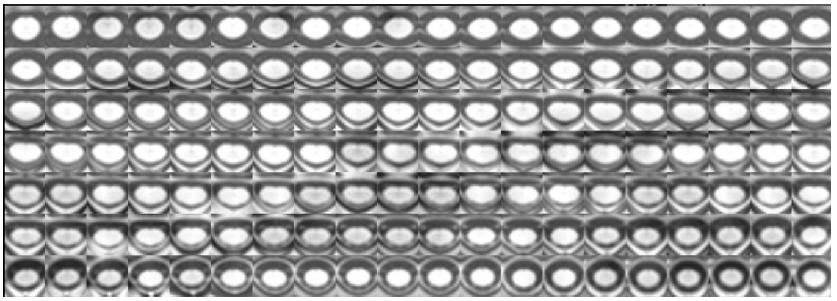

Figure 51: Quality control of the source target image (in our implementation this figure and figure 51 are superposed in a dynamic fashion

With this tool we are able to quickly see if the spine is being rotated correctly.

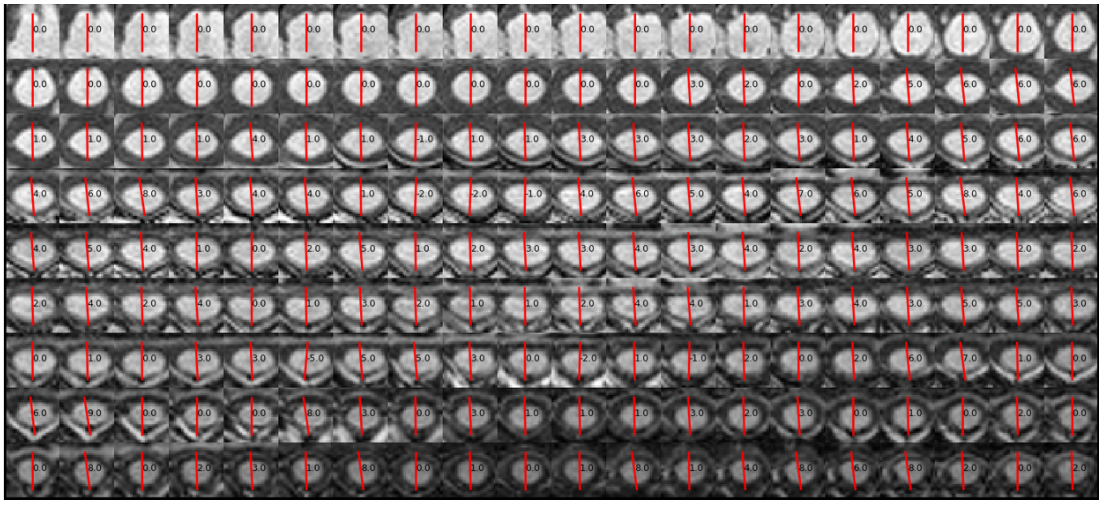

Figure 52: Quality control of the symmetry axis detected on the source image

With this tool we are able to quickly grasp the accuracy of the angles detected.

3.5.2 Quantitative evaluation

Now that we have a way of seing visually the result of our method, we will need to have quantitative results.

One way of doing so would be to have the ground truth[27] of the angles directly, however it is not advisable for 2 reasons :

- It would be really tiresome to assess manually the angle of a lot of images
- It would be quite subjective and not really reliable to assess those angles manually

For those reasons we have decided to evaluate our method by putting it in its global context : the rigid registration. We will try to evaluate the quality of the rigid registration with our method VS the quality of the registration with the PCA method[28]. We think this is relevant because :

- At the end, the goal is to improve the registration, so judging on this criterion seems reasonable
- It is easier to get a quantitative assessment that does not require ground truth, or at least ground truth that we don't have

The idea is to once again take advantage of the fact that we have a proper segmentation of the spinal cord.
We will compute the registration between the image and the corresponding atlas image[29] with PCA and our method. This registration will output a warping field allowing to warp the image to the atlas and the other way around.
We will then apply the same warping field to the segmentation of the image, giving us a registered segmentation. We can then compare this registered segmentation to the original segmentation of the atlas by any similarity metric we desire, for instance the Dice score [34], the Haussdorf distance [33] and so on.
It is much easier to assess quantitatively the difference between two segmentations (binary masks) than it is between two images (here the registered image and the atlas). This method is also described in the paper [7] as a "morphology-based" evaluation, which support the use of this method.

[27] In fact it will not really be a ground truth but rather a gold standard

[28] And also VS no rotation at all, only a translation, to see if there is even a benefit rotating the image

[29] If the image is for instance a T1w image, we will register it to the T1w atlas

The whole process is summarized figure 53.

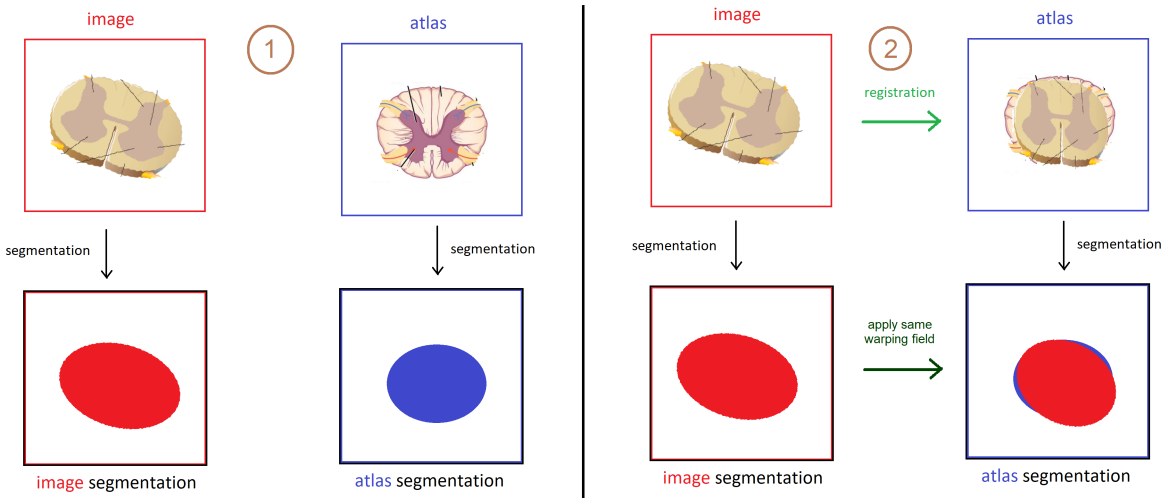

Figure 53: Schematic of the proposed evaluation of our method, in the end we compute a similarity metric between the red and blue ellipse

There are however a few flaws in this evaluation method that we need to think about :

- The segmentation of the atlas can be considered as ground truth but the segmentation of the image might not be totally accurate
- We are assessing only the global shape of the spinal cord that way, the interior of the spinal cord or the structure very close to it might be misregistered and we will not notice it
- We are dependant on the whole registration process, not only the rotation part (even if in our rigid registration case there is only a translation before)

Quantitative and qualitative evaluation can be complementary, we could localize in which image the metric has a bad score and check visually the symmetry axis or the registration to have more details. On the other way around we could check if bad visual registration or symmetry axis have a good or bad score and maybe investigate the why and how.

NB : When discussing with other colleagues, many of them asked us why we don't "simply rotate the image manually by a known angle and then compute the difference between the known angle and what the method found" as a way to assess quantitatively assess our method. The thing is that those manual rotations are not representative of the reality. When a subject tilts its head in the scanner, it will not

rotate its whole body, neither will it rotate only the spinal cord. The spinal cord will be rotated and the tissue around will be less and less affected by this rotation as we go further from the spinal cord[30], meaning this rotation is complex and influence the nearby tissue in a continuous fashion, meaning simply rotating the image is not a good way to evaluate the method.

Another method would be to have "important landmarks" labeled by an expert (or not) and evaluate the difference between those landmarks, rather than evaluating the segmentation, this will kind of compensate for the flaws we pointed, but will reacquire manual "expert" labelling. This approach has been suggested in [7].

3.6 Results of evaluation

The qualitative evaluation, although not being done with more than 20 subjects, has given promising results.
The PCA method is consistent and robust but often gives angles out of the a priori range, leading to angle being set by default to 0.
Our method on the other hand is more ambitious and often spot rotation of 1 or 2 degrees that PCA fails to capture, however this ambition leads to more abberant angles than the PCA method.
The automatic method seems to be a good compromise between the two, since it captures the robustness of the PCA when the spine is ellipsoïdal and tries to catch small variations in angles when the spinal cord is quasi-round.

For the quantitative evaluation, unfortunately the latest the results that we have ran to this day are not satisfying. They give the advantage to the PCA method over ours, surely because of its robustness. We could say that our method "takes more risks", but those risks are not rewarded by the Dice score.
Furthermore, in most case, just applying no rotation gives us better Dice score, meaning the utility of the rotation at this step is still to prove.

We wish however to say that we hadn't time to run the quantitative evaluation on the automatic method, which seemed the more promising of the 3.

Also, we have run he quantitative evaluation only with the Dice metric, this metric has its flaws and is a specific kind of metric.

[30]This fact also support our use of the Gaussian segmentation based weighting map

Further quantitative evaluation with the auto method and other metrics will be needed if we want to validate the benefit of our work.

4 Discussion

In this section we will try to take a step back and discuss what we have brought into solving the problem since the beginning.

4.1 Benefits of the method

As we have said before, the method that we developped seem more "ambitious" than the PCA method. It tries to capture small angle rotation, whereas the PCA is often grossly evaluating the orientation.
The method tries to combine the information present in the segmentation and the image.

We have demonstrated that our improvement effectively reduce the noise present in the auto-convolution of the histogram in Sun et al. method [3].

The automatic method, both in theory and in the qualitative evaluation gives satisfaction and we wish to prove its superiority in the future.

4.2 Limits of the method

One of the primary goals was to develop a method more robust than the PCA. As is, our method don't meet this goal because of its "adventurous nature", however it gives non-aberant angle most of the time (at least more than PCA) in the case of quasi-round spinal cord.
We can maybe see the limits of the base technique by Sun [11], because it was here used with images that have very few pixels (fewer than the tests images used in 1998, because we are talking about MRI of a really small part of the human body).

4.3 Avenues for improvements

We have a few things to suggest in improving our method or path to search for :

- Evaluating quantitatively the automatic method
- Trying other metrics than the Dice score
- Try to make the confidence score strategy work (maybe by mixing the 2 proposed score in an astucious way ?)
- Trying to implement and if possible improve other pixel-wise symmetry detection methods (This is very long but can be worth it, maybe a combination of 3 methods would give satisfying results)
- Right now the 2D slice are extracted following the inferior-superior direction, it could be relevant to extract 2D slice orthogonal to the spinal cord centerline
- Try other weighting by the segmentation than the gaussian one
- Implement a smarter strategy for outputing smooth angles along the inferior-superior direction than just smoothing at the end
- Try fine tuning all the hyper-parameters of the method

5 Conclusion

We have described in this report our objective for this research year abroad and give a methodological and scientific background on our work, by quickly describing MR imaging, the spinal cord and the global work of the laboratory.
We have then stated the problem in a formal way, and presented registration and symmetry detection algorithms. We then showed how we improved an existing method and adapted it to our case and what was the strategy in evaluating it.
Finally we drew a path for the future work coming from this research year by proposing tracks in improving and continuing this work.

6 Personnal conclusion

It was a great plaisure and a really interesting opportunity working in a foreign research laboratory. I have discovered a research system that is in some way different and in some way similar to the french research system. It was of great interest to work with people that are not only french-speaking or in the applied mathematics field in the way that it gives great insight about the whole discipline of medical imaging.
Finally I think that I have made progress in the many fields linked to my whole

internship, including being part of a research time for a long period.
I am definitely motivated into pursuing into a PhD and I am confident that this foreign research year has given me a more accurate idea about what pursuing a research activity really is.

7 Acknowledgments

I greatly thank all the members of the Neuropoly lab for welcoming me and helping me in my research. I also want to thank my supervisor Julien Cohen-Adad for being very receptive and giving great feedback about my work. Lastly I shall thank Louis L. and Guillaume M. for the very interesting discussions we had.

Figure 54: Neuropoly research team in May 2019

Bibliography

[1] A. Abragam, *The Principles of Nuclear Magnetism*, Oxford University Press, London, England, 1961

[2] Dwight G. Nishimura, *Principles of Magnetic Resonance Imaging*, Edition 1.2, August 2016, Chapter 1 to 7

[3] C. Sun and D. Si, *Fast Reflectional Symmetry Detection Using Orientation Histograms*, Real-Time Imaging, vol. 5, no. 1, pp. 63–74, Feb. 1999.

[4] Nógrádi A, Vrbová G, *Anatomy and Physiology of the Spinal Cord*, In: Madame Curie Bioscience Database [Internet]. Austin (TX): Landes Bioscience; 2000-2013. Available from: `https://www.ncbi.nlm.nih.gov/books/NBK6229/`

[5] *1,500 scientists lift the lid on reproducibility*, Nature 533, 452–454 (26 May 2016) doi:10.1038/533452a

[6] B. De Leener et al., *SCT: Spinal Cord Toolbox, an open-source software for processing spinal cord MRI data*, NeuroImage, vol. 145, pp. 24–43, Jan. 2017.

[7] L. Tang and G. Hamarneh, *Medical Image Registration: A Review*, Medical Imaging, p. 42.

[8] B. B. Avants, C. L. Epstein, M. Grossman, and J. C. Gee, *Symmetric Diffeomorphic Image Registration with Cross-Correlation: Evaluating Automated Labeling of Elderly and Neurodegenerative Brain*, Med Image Anal, vol. 12, no. 1, pp. 26–41, Feb. 2008.

[9] R. Bitar, G.Leung, R.Perng,et al., *MR pulse sequences: what every radiologist wants to know but is afraid to ask*, Radiographics26(2006) 513-537

[10] S.C. Joshi, M.I. Miller et al., *Landmark matching via large deformation diffeomorphisms*, IEEE Transactions on Image Processing Volume 9, pages 1357 - 1370

[11] C. Sun, *Symmetry detection using gradient information*, Pattern Recognition Letters, vol. 16, no. 9, pp. 987–996, Sep. 1995.

[12] Neil G Burnet et al., *Defining the tumour and target volumes for radiotherapy*, Cancer Imaging 4(2):153-61

[13] Anand Joshi et al., *A Framework for Brain Registration via Simultaneous Surface and Volume Flow*, inf Process Med Imaging. 2009; 21: 576–588.

[14] Pei Dong et al., *Efficient Groupwise Registration for Brain MRI by Fast Initialization*, Mach Learn Med Imaging. 2017

[15] N. J. Tustison and B. B. Avants, *Explicit B-spline regularization in diffeomorphic image registration*, Front Neuroinform, vol. 7, Dec. 2013.

[16] J. Cohen-Adad et al., *Slice-by-slice regularized registration for spinal cord MRI: SliceReg*, ISMRM 2015

[17] `http://stnava.github.io/ANTs/`

[18] G. Loy and J.-O. Eklundh, *Detecting Symmetry and Symmetric Constellations of Features*, Computer Vision – ECCV 2006, vol. 3952

[19] R. Scognamillo, G. Rhodes, C. Morrone, and D. Burr, *A feature-based model of symmetry detection.*, Proc Biol Sci, vol. 270, no. 1525, pp. 1727–1733, Aug. 2003.

[20] `https://en.wikipedia.org/wiki/Symmetry_(geometry)`

[21] `https://en.wikipedia.org/wiki/Atan2`

[22] `https://scienceatyourdoorstep.com/2014/09/08/precession/`

[23] `https://en.wikipedia.org/wiki/Nuclear_magnetic_resonance`

[24] `https://case.edu/med/neurology/NR/MRI\%20Basics.htm`

[25] `https://www.scienceabc.com/humans/whats-the-role-of-spinal-cord-in-your-overall-well-being.html`

[26] `https://www.christopherreeve.org/living-with-paralysis/health/how-the-spinal-cord-works`

[27] `https://en.wikipedia.org/wiki/Image_registration`

[28] J. B. A. Maintz and M. A. Viergever, *A Survey of Medical Image Registration*, p. 37.

[29] https://www.studyblue.com/notes/note/n/medical-terminology-body-planes-regions/deck/18906006

[30] http://fisica.unipv.it/Mihich/FM/7-PDF_1_sect05.pdf

[31] B. B. Avants, P. T. Schoenemann, and J. C. Gee, *Lagrangian frame diffeomorphic image registration: Morphometric comparison of human and chimpanzee cortex*, Medical Image Analysis, vol. 10, no. 3, pp. 397–412, Jun. 2006.

[32] G. Loy and J.-O. Eklundh, *Detecting Symmetry and Symmetric Constellations of Features*, Computer Vision – ECCV 2006, vol. 3952, A. Leonardis, H. Bischof, and A. Pinz, Eds. Berlin, Heidelberg: Springer Berlin Heidelberg, 2006, pp. 508–521.

[33] D. P. Huttenlocher, G. A. Klanderman, and W. J. Rucklidge *Comparing images using the Hausdorff distance*, IEEE Transactions on Pattern Analysis and Machine Intelligence, vol. 15, no. 9, pp. 850–863, Sep. 1993.

[34] https://en.wikipedia.org/wiki/S\%C3\%B8rensen\%E2\%80\%93Dice_coefficient

[35] H. Akbar, K. Hayat, N. ul Haq, and U. I. Bajwa, *Bilateral Symmetry Detection on the Basis of Scale Invariant Feature Transform*, PLoS One, vol. 9, no. 8, Aug. 2014.

[36] D. G. Lowe, *Object recognition from local scale-invariant features*, in Proceedings of the Seventh IEEE International Conference on Computer Vision, Kerkyra, Greece, 1999, pp. 1150–1157 vol.2.

[37] A. Migalska and J. Lewis, *An information theoretic approach to reflectional symmetry detection*, in 2015 International Conference on Image and Vision Computing New Zealand (IVCNZ), Auckland, New Zealand, 2015, pp. 1–6.

[38] https://people.cs.umass.edu/~elm/Teaching/Docs/mutInf.pdf

[39] https://en.wikipedia.org/wiki/Principal_component_analysis